# Inter-Ring Torsions in *N*-Phenylmaleimide and Its *o*-Halo Derivatives: An Experimental and Computational Study

**Christopher W. Miller and Charles E. Hoyle**

*School of Polymers and High Performance Materials, The University of Southern Mississippi, Hattiesburg, Mississippi 39406-0076*

**Edward J. Valente* and David H. Magers**

*Department of Chemistry, Mississippi College, Clinton, Mississippi 39058-4036*

**E. Sonny Jönsson**

*Becker-Acroma, S19502 Märsta, Sweden*

*Received: February 15, 1999; In Final Form: June 8, 1999*

Structures of *N*-phenylmaleimide and its *o*-halophenyl derivatives have been determined in the solid state and show the angle between the phenyl and pyrolinyl ring planes to vary from 49.5° to 83.9° with increasing values for compounds with the larger ortho halophenyl substituents (H < F ≲ Cl ≲ Br < I). Experimental torsions and trends in the series are supported by semiempirical AM1 and ab initio SCF, DFT, and MP2 calculations. Calculations (AM1) on *N*-phenylmaleimide modeling the torsional deformation between the rings show that the barrier to planarity has a lower energy than that through a perpendicular conformation. In its *o*-halo derivatives, molecular planarity is not possible, and torsional deformation proceeds through the perpendicular conformation with diminishing, possibly vanishing, barriers with increasing halogen size. For chloro, bromo, and iodo derivatives, twisted ground-state molecular conformations reside in broad minima essentially centered around the perpendicular conformations. The unusually strong, longer wavelength electronic bands observed in the solution spectra of the series were modeled by Zindo/S CIS computations at the optimum AM1 molecular geometries. The observed lower energy (285−305 nm) band for the parent through the *o*-bromo derivative appears to arise from a $\{n_{\perp}(O,N); \pi\ (phenyl)\} \rightarrow \pi^*$(maleimide) transition. The next higher energy (250−285 nm) band appears to be essentially a phenyl $\pi \rightarrow \pi^*$ transition. In the *o*-iodo derivative, a phenyl $\pi \rightarrow \sigma^*$ (C−I) transition appears to contribute to the longer wavelength band. Trends in the observed electronic spectra in acetonitrile within the series of compounds accord roughly with the results of the computations.

## 1. Introduction

Substituted maleimides and citraconimides are convenient monomers for the production of thermally cured and/or photocured polymers with a wide range of properties and applications. Ultraviolet-curable mixtures containing *N*-arylmaleimides in combination with other monomers and acrylic systems have been studied for coatings applications. *N*-Arylmaleimides have been found to function as both photoinitiators and comonomers in ultraviolet-curable formulations which polymerize by free-radical mechanisms. Although planar *N*-arylmaleimides do not appear to initiate polymerization upon direct excitation, ortho-substituted (i.e., twisted) *N*-arylmaleimides appear to be relatively efficient photoinitiators upon direct excitation in the presence of a hydrogen atom donor synergist. The mechanism of initiation is believed to occur through free-radical production via hydrogen atom abstraction reactions similar to those observed with benzophenone.[1−5] The properties of the resulting polymers are not thought to be significantly modified by the presence of the *N*-arylmaleimides where they are used principally as the photoinitiator since they typically comprise only a few parts per hundred (1−5 wt % in the precured formulation) in the final polymers.[6−8] In a study examining the electronic absorption features of substituted maleimides,[9] calculations on N-substituted maleimides led to assignments of the longer wavelength bands in the solution spectra to a carbonyl $n \rightarrow \pi^*$ transition, even though this band is considerably stronger than usual. Band intensities were strengthened, it was argued, by mixture of the $n \rightarrow \pi^*$ with a maleimide $\pi \rightarrow \pi^*$ transition. Two effects were postulated that bear on the spectra of *N*-phenylmaleimides. Either the $n \rightarrow \pi^*$ band could receive further intensification through overlap with the phenyl $\pi$ system at low inter-ring torsional angles, or the $\pi \rightarrow \pi^*$ band could be enhanced by oxygen 2p interaction with the occupied phenyl $\pi$ orbitals which should be maximal where the rings are perpendicular. A compromise seemed to be the best explanation for the observed spectra and trends, with the phenyl ring of *N*-phenylmaleimide serving as a bulky substituent preserving the planarity of the maleimide nitrogen and the purity and weakness of the $n \rightarrow \pi^*$ transition. Consistent with these assignments, little difference was detected in the spectra of *N*-phenylmaleimides and a few p-substituted derivatives. A later report questioned this $n \rightarrow \pi^*$ assignment.[10]

It is obvious that the inter-ring angle in *N*-phenylmaleimides can be affected by *ortho* substitution. These structural modifications may provide useful information on the resulting electronic

* Author to whom correspondence should be addressed. E-mail: valente@mc.edu.

10.1021/jp9905474 CCC: $18.00 
Published on Web 07/16/1999

spectra of maleimides and their assignment. The present contribution describes structural, spectroscopic, and theoretical studies of *N*-(*o*-halophenyl)maleimides, where the halogens are fluorine, chlorine, bromine, and iodine, and compares them with similar examinations of the parent unsubstituted molecule. Halo derivatives were synthesized, and together with the unsubstituted parent compound, their solid-state structures were determined by single-crystal X-ray diffraction. These structures were compared with the most stable conformations modeled for the gas-phase molecules by semiempirical AM1 and ab initio computations. Additionally, we have calculated the energetic dependence of the rotation of the rings with respect to each other. For substituents larger than fluorine, planarity should be prohibited along the path of inter-ring torsional distortion due to steric interactions between the imide oxygens and the *ortho* substituent. Instead, these molecules should undergo distortions within the maleimide and/or phenyl moieties. Electronic spectra of the molecules from their ground to first excited states have been calculated based on the minimum energy geometries, and these have been compared with the solution spectra of the substances in several solvents.

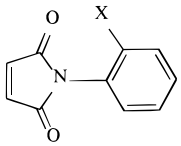


X = H, F, Cl, Br, I
(**1**) (**2**) (**3**) (**4**) (**5**)

## 2. Results and Experimental Section

**2.1. Syntheses and Spectroscopy.** Solvents for spectroscopy were purchased from Burdick and Jackson and were of the highest available purity. *N*-Phenylmaleimide was obtained from Aldrich Chemical company and recrystallized from benzene. Ultraviolet spectra were obtained in a 1.0 cm cell on Perkin-Elmer Lambda-5 and Cary 500 spectrometers at ambient temperature. Differential scanning calorimetry (DSC) was performed on a Shimadzu DSC-50; samples with 2.0 mg mass were sealed in aluminum cells and heated at 10 °C/min under a nitrogen atmosphere; 99.9999% tin and indium were used for standards for fusion temperatures and heats of fusion.

*Haloaryl-Substituted N-Phenylmaleimides.* These were prepared following a general procedure for the synthesis of maleimides. This method involves two steps beginning with reaction of a 2-haloaniline with maleic anhydride in ethyl ether to produce an intermediate 2′-halophenylamide of maleic acid in near quantitative yield. After thoroughly drying the amic acid, it was cyclized to the imide by refluxing its solution in toluene and dimethyl sulfoxide in the presence of a catalytic amount of concentrated sulfuric acid. Water was removed through the water/toluene azeotrope, and excess toluene was then removed by distillation. The product imide was recovered in near quantitative yield after precipitation by addition of water to the dimethyl sulfoxide solution and filtration. Product imides were then thoroughly dried. Samples suitable for crystallography were obtained from various solvents. Melting points and heats of fusion for the compounds were determined from DSC peaks and integration of fusion endotherms (K, kJ/mol): (H) 364.4, −19.0; (F) 347.8, −19.2; (Cl) 349.6, −20.1; (Br) 359.2, −18.8; (I) 383.8, −18.6.

Ultraviolet−visible spectra from 250 to 600 nm were recorded for solutions of each *N*-arylmaleimide in acetonitrile, dichloromethane, and chloroform. No absorptions were seen above 425 nm. Concentrations of the solutions in acetonitrile for the spectra displayed in Figure 1 were [mol($\times 10^{-3}$)/L]: H, 1.10; F, 1.37; Cl, 1.05; Br, 1.05; I, 0.956. Concentrations of the solutions of *N*-(2′-fluorophenyl)maleimide in acetonitrile, dichloromethane, and chloroform for the spectra displayed in Figure 2 were [mol($\times 10^{-3}$)/L] 1.37, 1.49, 1.05, respectively. These showed the following principal maxima $\lambda$ (nm), $\epsilon$ ($M^{-1}$ cm): in acetonitrile, 262, 1316; 293, 513; in dichloromethane, 263, 1377; 299, 507; in chloroform, 263, 1502; 300, 619. The longer wavelength broad maximum had the following characteristics in acetonitrile, $\lambda$ (nm), $\epsilon$ ($M^{-1}$ cm): (H) 306, 480; (F) 296, 367; (Cl) 286, 491; (Br) 286, 487; (I) shoulders below 280, unmeasured. The higher peak of the shorter wavelength multi-peaked maxima had the following characteristics in acetonitrile, $\lambda$ (nm), $\epsilon$ ($M^{-1}$ cm): (H) 259, 379; (F) 262, 1316; (Cl) 266, 678; (Br) 266, 729; (I) shoulder at 270, 1017.

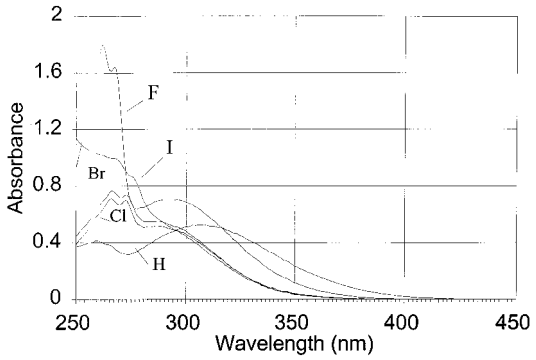


**Figure 1.** Ultraviolet spectra of *N*-phenylmaleimide and its 2′-halo derivatives in acetonitrile.

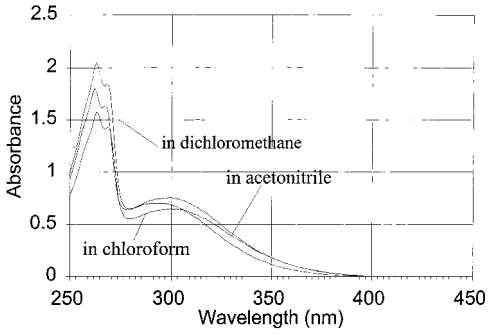


**Figure 2.** Ultraviolet spectra of *N*-(2′-fluorophenyl)maleimide in acetonitrile, dichloromethane, and chloroform.

**2.2. Crystallography.** Table 1 contains an abridged summary of the crystal data and data collection parameters. Data were collected on a Siemens *R*3*m*/v automated diffractometer with graphite monochromatized Mo Kα radiation ($\lambda$ = 0.71073 Å) using $\omega$ scans of width 2.0°. Three standards were monitored periodically (every 197 reflections). Reflection data were corrected for Lorentz, polarization and deterioration effects but not for absorption. Absorption effects are more serious in **4** and **5**, as can be seen from the residuals in electron density in the final Fourier maps. The effects do not render suspect the molecular conformations. Positions and anisotropic vibrational parameters were refined for all non-H atoms by full-matrix least-squares minimizing differences in $F^2$. Hydrogens were assigned calculated positions and allowed to ride on their attached atoms with isotropic vibrational factors equal to 120% of the equivalent isotropic vibrational factor of the attached atom. Fluorines in one of the two molecules in the asymmetric unit of **2** were disordered and appear in both ortho positions with the major conformer having an occupancy of 0.658(6). A more extensive tabulation of relevant crystallographic experimental information, and the positions of the non-hydrogen atoms and their isotropic equivalent vibrational factors, are given in the Supporting

**TABLE 1: Abbreviated Crystal Data for *N*-Phenylmaleimide (1) and *o*-Halo Derivatives (2−5)[a]**

| compound | 1 | 2 | 3 | 4 | 5 |
|---|---|---|---|---|---|
| formula | $C_{10}H_7NO_2$ | $C_{10}H_6FNO_2$ | $C_{10}H_6ClNO_2$ | $C_{10}H_6BrNO_2$ | $C_{10}H_6INO_2$ |
| formula weight | 173.17 | 191.16 | 207.61 | 252.07 | 299.06 |
| specimen dimensions, mm | 0.6, 0.4, 0.3 | 0.7, 0.4, 0.3 | 0.7, 0.4, 0.2 | 0.4, 0.2, 0.2 | 0.4, 0.6, 0.4 |
| crystal system | monoclinic | monoclinic | monoclinic | monoclinic | monoclinic |
| space group | $P2_1/n$ | $P2_1/n$ | $P2_1/c$ | $P2_1/c$ | $P2_1/c$ |
| temperature, K | 173.17 | 292(2) | 293(2) | 293(2) | 292(2) |
| cell constants: | | | | | |
| *a*, Å | 3.971(1) | 11.373(4) | 10.582(5) | 7.796(1) | 11.191(8) |
| *b*, Å | 10.744(3) | 6.524(3) | 12.599(5) | 12.606(3) | 10.437(10) |
| *c*, Å | 19.464(7) | 23.694(15) | 7.578(3) | 10.629(3) | 9.184(7) |
| α, ° | 90 | 90 | 90 | 90 | 90 |
| *β*, ° | 93.20(2) | 97.21(4) | 110.01(3) | 110.61(2) | 104.04(6) |
| *γ*, ° | 90 | 90 | 90 | 90 | 90 |
| cell volume, Å$^3$ | 829.1(4) | 1744.2(15) | 949.4(7) | 977.8(4) | 1040.7(14) |
| formula units/cell | 4 | 8 | 4 | 4 | 4 |

[a] Estimated standard deviations in parentheses.

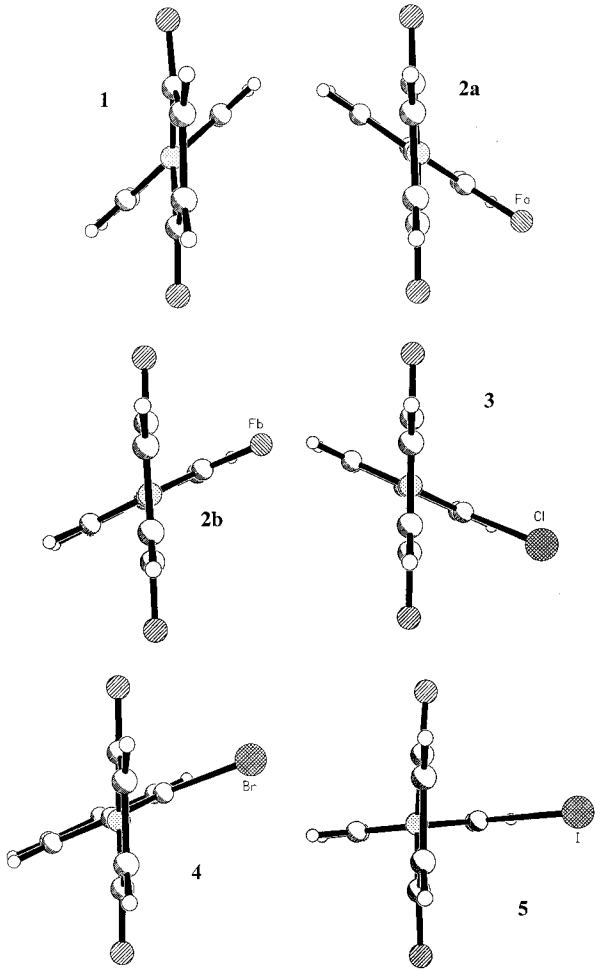


**Figure 3.** Projections of the crystal structures of **1**−**5** along the inter-ring bond.

Information. Projections of the structures, including both molecules of the fluoro derivative, are given in Figure 3. Atomic scattering factors were from The International Tables for Crystallography;[11] programs used were SHELXS-86 [12] and SHELXL-97.[13]

**2.3. Calculations.** *N*-Phenylmaleimide and its ortho halogen derivatives were modeled within the semiempirical AM1[14] method to calculate the minimum energy conformers using Hyperchem[15] and PC-Spartan[16] program packages. The torsion angle ($\tau$) described by $C_{ortho}-C_{ipso}-N-C_{carbonyl}$ was constrained to values descriptive of rotamers of the molecules, and the energy was minimized by adjusting all other structural degrees of freedom. Table 2 contains the results of the unconstrained minimum energy conformers and the constrained energies associated with the perpendicular ($\tau$ − 90°) conformers. For rotamers of the substituted molecules with $\tau < \tau_{min}$, structures in which inter-ring torsion angles tend toward coplanarity, distortions of the molecular structures involving deviations from planarity in both the phenyl and pyrolinyl rings were noted. A planar model, of course, cannot be accomplished where the ortho halogen was larger than fluorine. Calculated energies modeling the inter-ring torsional distortions are therefore more useful in an examination of the broad and shallow region before distortions from ring planarity occur. Rotamer forms for each substituted molecule were calculated nevertheless between the arbitrary limits of $\tau$ − 0° to 90°; these limiting values are also given in Table 2.

**TABLE 2: Semiempirical AM1 Calculated Minimum Energy Rotational Conformers and Calculated Relative Energies for Rotamers of *o*-Halo *N*-phenylmaleimides**

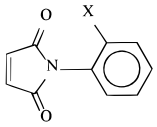


| compound, X | $\tau$[a] at $E_{min}$ (calcd, deg) | $\Delta E$ ($\tau \approx 0°$)[b] (calcd, kcal/mol) | $\Delta E$ ($\tau \approx 90°$) (calcd, kcal/mol) |
|---|---|---|---|
| H | 26 | +0.5 | +2.2 |
| F | 49 | +3.1 | +0.12 |
| Cl | 79 | +8.6 | <0.005 |
| Br | 85 | +10.3 | <0.01 |
| I | 90 | +11.2 | minimum |

[a] $\tau$ defined as $C_o-C_i-N-C(=O)$ angle. [b] $\tau \approx 0$ is not a planar structure for X = halogen.

Electronic spectra were computed by the Zindo/S method[17,18] using a singly excited configuration interaction (CIS) at the AM1 ground-state molecular geometries. A summary of the transition frequencies and oscillator strengths for the bands above 250 nm is given in Table 3. Assignments of the transitions for the longer wavelength band are also given in Table 3. For the bands in the range 250−285 nm, calculations predicted the following transitions [nm, strength, molecular orbital assignment (see Figure 4), where H = HOMO, L = LUMO]: for the unsubstituted compound, 285.3; 0.003; (H, H − 2) → L; 270.2, 0.008, (H, H − 1) → (L + 1, L + 2); for *o*-fluoro derivative, 277.2, 0.002, (H − 1, H) → (L, L + 1); 269.8, 0.015 (H, H − 1) → (L + 1, L + 2); for *o*-chloro derivative, 271.1, 0.001, H → L + 1; for *o*-bromo derivative, 269.3, 0.002, H → L + 1; for

**TABLE 3: Calculated Singlet Electronic Spectral Features at Gas-Phase Minimum Energy Conformations**

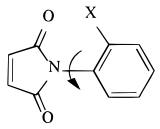


| compound X | torsion angle (AM1) (deg) | longer wavelength transition (ground → excited state) | Zindo/S transitions[a] 285−305 band $\lambda$ (nm) | 285−305 band $I$ (Debye) | 250−285 bands $\lambda$ (nm) | 250−285 bands $I$ (Debye) |
|---|---|---|---|---|---|---|
| H | 26 | $\{n_\perp(O,N) + \pi_{Ph}\} + \{n_\perp(N,O) + \sigma\} \rightarrow \pi^*_{Mal}$ | 303.8 | 0.017 | 285.3 | 0.003 |
| | | | | | 270.2 | 0.008 |
| F | 49 | $\{n_\perp(N,O) + \sigma\} \rightarrow \pi^*_{Mal}$ | 291.4 | 0.006 | 277.2 | 0.002 |
| | | | | | 269.8 | 0.015 |
| Cl | 79 | $\{n_\perp(O,N) + \pi_{Ph}\} \rightarrow \pi^*_{Mal}$ | 287.1 | 0.007 | 271.1 | 0.009 |
| Br | 85 | $\{n_\perp(O,N) + \pi_{Ph}\} + \{n_\perp(O,N) + \pi_{Ph}\} \rightarrow \pi^*_{Mal}$ | 292.8 | 0.003 | 269.3 | 0.002 |
| I | 90 | $\{n_\perp(O,N) + \pi_{Ph}\} \rightarrow \{\pi^*_{Ph} + \sigma(C-I)\}$ | 286.7 | 0.010 | 250.5 | 0.0003 |

[a] Determined at AM1 minimum energy geometries.

*o*-iodo derivative, 250.5, 0.0003, (H − 1, H) → L + 1; 242.4, 0.0001, H → L.

Finally, optimized equilibrium geometries were computed for *N*-phenylmaleimide and its *o*-halophenyl derivatives at the ab initio levels of SCF theory, density functional theory (DFT), and second-order perturbation theory (MP2) using the Gaussian98 program suite.[19] The DFT employed was Becke's three-parameter hybrid functional[20] using the LYP correlation functional.[21,22] Optimized torsion angles from these calculations are reported in Table 4. Molecular geometries using lower basis sets (not tabulated) showed convergence in each theory; the final 6-31G(d,p) basis was employed on all atoms.

## 3. Discussion

**3.1. Solid-State Structures and Geometry Calculations.** *N*-phenylmaleimide and its 2′-halophenyl derivatives are unsolvated in their solids. The structures of the five *N*-phenylmaleimides found in the solid state are shown in Figure 3 in projection down the inter-ring axis. Torsion angles across the N−C bond joining the rings are given in Table 4, and generally increase with the size of the ortho halogen substituent on the phenyl ring. Molecular volume in the solids increases steadily from 207.3 Å$^3$ for *N*-phenylmaleimide to 260.2 Å$^3$ for *N*-(2′-iodophenyl)maleimide, an indication of the increasing molecular size to which the halogen substituent contributes. In all of the computations, a trend toward wider inter-ring angles as halogen size increases is observed. Table 4 shows that the inter-ring torsions calculated by both AM1 and SCF methods differ from the experimental values more than that modeled by the two higher levels of theory. While the torsion angles determined at the DFT-B3LYP and MP2 levels were consistently closer to the experimental values, the AM1 level was chosen to model the rotational energy surface about the inter-ring angle.

Rings in *N*-phenylmaleimide (**1**) in the solid state are twisted relative to each other by 49.5° (Table 4). Calculations (AM1) on isolated *N*-phenylmaleimide show a minimum for a rotamer with an inter-ring dihedral angle of 26.4°. The rotational energy surface is rather broad and shallow, however, rising only 0.5 kcal/mol for a planar conformation and 2.2 kcal/mol for a perpendicular conformation. The energies of the conformers with inter-ring dihedral angles from planar to 52° lie within 1 kcal/mol of the conformational minimum. This suggests that, at room temperature, nearly all inter-ring rotational conformers are accessible to the molecule, and the rotamer present in the solid state is susceptible to the molecular environment in the crystal.[23]

Crystals of *N*-(2′-fluorophenyl)maleimide (**2**) contain two independent molecules in the asymmetric unit with different inter-ring dihedral angles averaging 60.5°. AM1 calculations on **2** show minimum energy rotamer with an inter-ring dihedral angle of 49.0°, and the barrier to conformational ring twisting is now higher at the planar form (+3.1 kcal/mol) than at the perpendicular form (+0.12 kcal/mol). As for **1**, the rotational energy surface is calculated to be broad and shallow with the energy for conformers having inter-ring dihedral angles from 90° (perpendicular) to 30° lying within 1 kcal/mol of that for the conformational minimum. Molecules of *N*-(2′-chlorophenyl)-maleimide (**3**) in the crystal show an inter-ring dihedral angle of 66.1°, while the calculated minimum energy rotamer has an inter-ring dihedral angle of 79° at the AM1 level of theory. The barrier to conformational ring twisting rises considerably as the conformation is constrained to smaller inter-ring twist angles. The barrier to a perpendicular conformational interconversion essentially disappears as the energy difference between that for the rotational minimum structure and the perpendicular conformer becomes less than 0.01 kcal/mol. The rotational energy surface is calculated to be broad and very shallow with rotamers having inter-ring dihedral angles from 90° (perpendicular) to 45° within 1 kcal/mol of the conformational minimum. Bromo (**4**) and iodo (**5**) phenylmaleimide derivatives in the solid state are found in conformations with inter-ring torsions of 71° and 84°, respectively. AM1 calculations on the isolated molecules show that the minimum energy conformers are above 80° and that these systems also have essentially no torsional barrier at the perpendicular conformation. The potential function is not as broad as with the lower halogen homologues , with rotational conformers within 1 kcal/mol of the lowest energy having dihedral angles of 55−90° for the bromo analogue, and 58−90° for the iodo analogue. These results are consistent with the increasing steric bulks of the larger halogens which precipitate significant intramolecular repulsions on torsion of the inter-ring C−N bond. In each case **2**−**5**, the conformations adopted by the molecules in the crystals have energies calculated to be less than 1 kcal/mol from that for the calculated minimum energy structure, and the differences can to some extent be associated with intermolecular packing interactions.

While the barrier to the perpendicular conformation essentially disappears for the larger ortho halogen derivatives, calculations show that, as their inter-ring torsion angle is reduced around the inter-ring C−N bond, molecular distortion takes place. Two distortions begin to appear as the conformational energies exceed 1 kcal/mol for the chloro, bromo, and iodo analogues: (a)

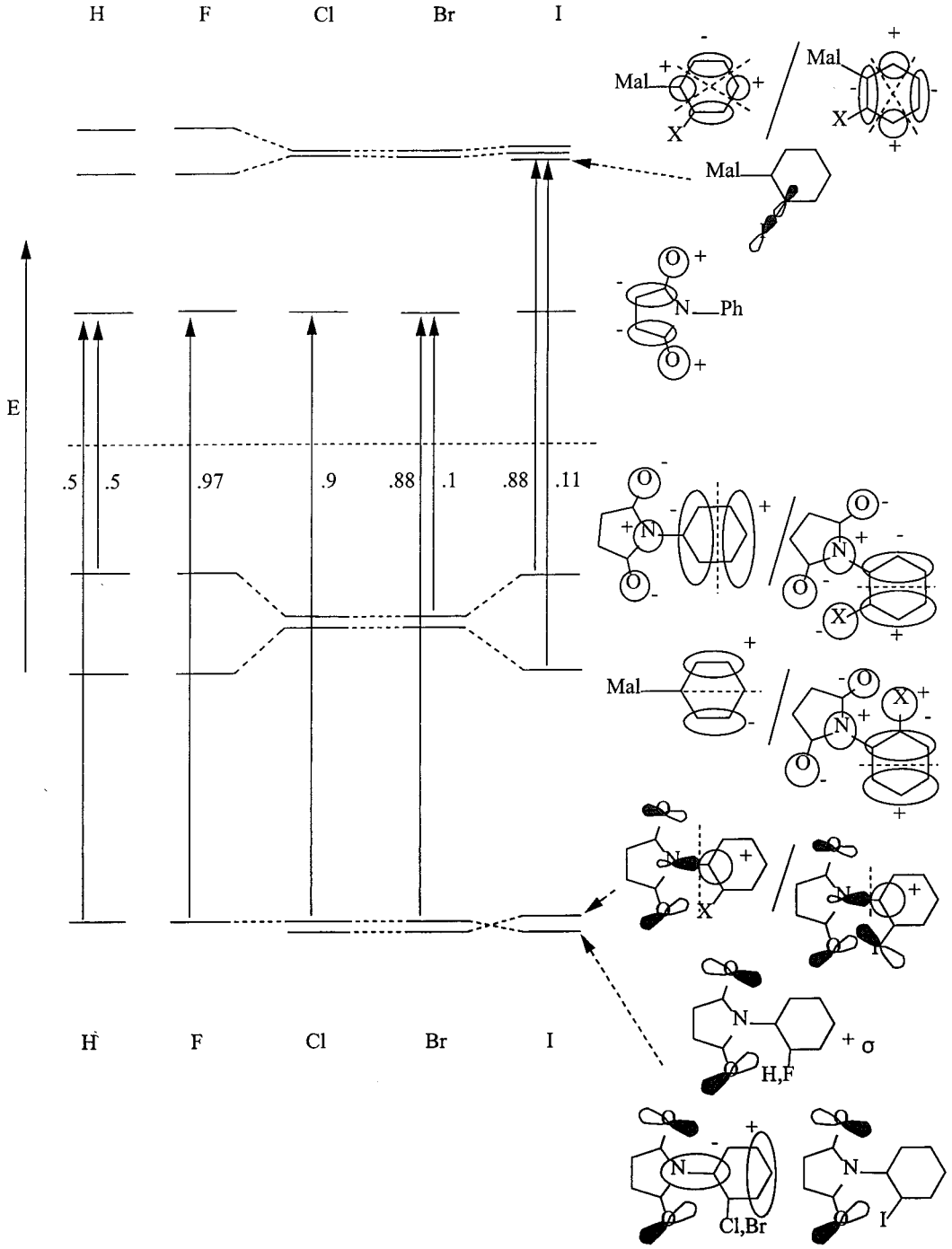


**Figure 4.** Ordering and major molecular orbital features for the frontier molecular orbitals and Zindo/S long-wavelength singlet transitions and weightings for *N*-phenylmaleimide and its *o*-halo derivatives. (Views are from above the phenyl rings except for the LUMO and show the upper p-lobes. Ph = phenyl/o-substituted phenyl; Mal = maleimide.)

pyramidalization of the nitrogen and (b) bending of the imide carbonyl from the 5-ring with simultaneous bending of the C−X group from the phenyl plane. Each of these becomes greater as the torsion angle $C_o-C_i-N-C(=O)$ is decreased. Planar structures are not possible for these larger halogen derivatives because the covalent radius of the halogen would enclose that of the imide carbonyl oxygen.

**3.2. Ultraviolet Spectra and Calculations.** In the ultraviolet spectra of *N*-phenylmaleimide and its ortho fluoro, chloro, and bromo derivatives above 250 nm, two principal features are observed in each: a broad absorption at or below 300 nm, and a second band from 250 to 285 nm (Figure 1). The higher energy band has diffuse vibrational fine structure in the halo derivatives. In the *o*-iodo derivative, the absorption spectrum is somewhat distinctive and suggests a significant overlap of these two bands and/or the presence of some other absorption. A small hypsochromic shift in both bands is observed generally for the spectra in acetonitrile relative to those observed in less polar solvents. The effect is shown in Figure 2 for *N*-(2′-fluorophenyl)-maleimide. Within the series of compounds, the longer wavelength band shifts to higher energy on *o*-halo substitution of the phenyl ring relative to the *N*-phenylmaleimide with the extent of the shift in the order I > Br > Cl > F. This band has been ascribed to an imide $n \rightarrow \pi^*$ transition by Matsuo.[6] Features of the shorter wavelength band shift to lower energy with substitution in the same order, leading to the somewhat unusual features

**TABLE 4: Inter-ring Torsion Angles (Degrees) from Semiempirical and ab Initio [Level: 6-31G(d,p)] Minimum Energy Conformers Compared to the Experimental Crystallographic Values**

| compound (o-substituted) | theory[a] | | | | X-ray experiment |
|---|---|---|---|---|---|
| | AM1 | SCF | DFT-B3LYP | MP2 | |
| H | 26 | 52.7 | 39.8 | 44.3 | 49.5 |
| F | 49 | 69.5 | 56.2 | 56.4 | 54.2, 66.8[b] |
| Cl | 79 | 87.6 | 71.2 | 67.6 | 66.1 |
| Br | 85 | | | | 71.1 |
| I | 90 | | | | 83.9 |

[a] Vacancies not modeled due to basis sets limitations. [b] Two conformers in the crystal.

in *N*-(2′-iodophenyl)maleimide which might represent overlap of bands. The intensity of the longer wavelength band seems too strong to be purely an n → $\pi^*$ transition, and that of the shorter wavelength band seems to be too weak to be purely a $\pi \rightarrow \pi^*$ transition.

Gas-phase electronic spectra for the series have been calculated by the Zindo/S CIS method at the AM1 minimum energy conformers. The results associated with the lowest energy transition is illustrated in Figure 4 which depicts the six or seven frontier molecular orbitals for each compound in the series. The lowest unoccupied molecular orbital in all members of the series is localized on the maleimide ring and may be described as having $\pi^*$(C═C) and $\pi^*$(C═O) character. Above this in energy, the next two are $\pi^*$ orbitals localized on the phenyl rings and each having two local perpendicular nodal planes. These two differ somewhat in energy in the parent and *o*-fluoro compounds, but have nearly the same energy in the rest of the series. In the *o*-iodo derivative, a $\sigma^*$(C−I, 2p−5p) orbital becomes nearly equal in energy to the $\pi^*$(phenyl) orbitals. In the occupied regime, the two highest occupied molecular orbitals have $n_\perp$(O,N,X) + $\pi$(phenyl) character, each with one local perpendicular phenyl nodal plane. These two differ somewhat in energy in the parent, *o*-fluoro, and *o*-iodo compounds, but have nearly the same energy in the *o*-chloro and *o*-bromo derivatives. Below this, each compound has a $n_\perp$(O,N) orbital which additionally has significant $\sigma$(C−C, C−N, C−H) character for the parent and the *o*-fluoro compounds, changing to $\pi$(C−N) and $\pi$(phenyl) character for the *o*-chloro and *o*-bromo derivatives and modifying further to $\pi$(C−N) and $\pi$(phenyl) character in the *o*-iodo derivative. These are depicted in Figure 4.

Beginning with AM1 molecular geometries, the electronic spectra were calculated for excited singlets with Zindo/S configuration interaction limited to single excitation (CIS) out of the Hartree−Fock ground states for each member of the series. The long-wavelength band assignments are given in Figure 4, and for the parent and three lightest *o*-halo derivatives involves a transition from an orbital with $n_\perp$(O,N) character to the $\pi^*$(maleimide) orbital (LUMO). The transition originates from a mixture of orbitals having $n_\perp$(O,N) and $\pi$(phenyl) character (HOMO) in the parent and *o*-bromo cases. The lower energy orbital in this transition decreases in $\sigma$ and increases in $\pi$ character as the inter-ring angle increases. In the *o*-chloro and *o*-bromo cases, a second orbital with $n_\perp$(O,N) and $\pi^*$(C−N) character also contributes. The nonbonded character of the longer wavelength transitions is supported by the hypsochromic shift in this band observed in the spectra of the *o*-fluoro derivative upon progression to more polar solvents. A change is predicted for the lower energy bands of the *o*-iodo derivative. The long-wavelength transition appears from higher occupied molecular orbitals with $n_\perp$(O,N) and $\pi$(phenyl) character to an unoccupied one with $\sigma$(C−I, 2p−5p) character.

A comparison between the solution (Figure 1) and calculated spectra (Table 3) provides some qualitative agreement. Ignoring for the moment the *o*-iodo derivative, two important features are seen in the spectra above 250 nm for *N*-phenylmaleimide and its three lighter *o*-halophenyl derivatives. Calculations predict two (for Cl and Br derivatives) or three (for the parent and F derivative) transitions in the same range. The oscillator strengths of the intermediate band in the parent and fluoro derivative are very small, leaving essentially two important features in each case. The lower energy bands are calculated to shift slightly to shorter wavelength in the halogen-substituted systems in the order H < F < Cl ≈ Br, and the solution spectra of the series follow this trend. The next higher of the two observed ultraviolet bands in the solution spectra are found at 260−270 nm. Calculations suggest that these next highest intensity bands have $\pi \rightarrow \pi^*$ (phenyl) character and should remain at 270 nm for H through Br and that the oscillator strength for the fluoro derivative should be larger than the others. Both the position and intensities of the observed bands are roughly in agreement with the calculations.

For the *o*-iodo derivative, a change is seen in the observed spectrum (Figure 1) in which the stronger, shorter wavelength band appears to shift slightly to longer wavelength compared to the lighter halogen derivatives, and to intensify. Computations suggest that this may be accounted for by a change in the transition responsible for the longer wavelength absorption compared to the parent and lighter halogen derivatives. The longer wavelength band seems to be due to a $\pi_{Ph} \rightarrow \sigma^*$(C−I, 2p−5p) transition and to be accompanied by an increase in intensity and shift to slightly longer wavelength compared to the other *o*-halo derivatives. These predictions are in accord with the spectrum of the *N*-(*o*-iodophenyl)maleimide.

## 4. Conclusions

The structures of *N*-phenylmaleimide and the *o*-halo-*N*-phenylmaleimides (fluoro, chloro, bromo, and iodo) have been determined and show that the inter-ring torsion increases with increasing steric size of the halogen. Semiempirical AM1 and several ab initio calculations generally agree with the solid-state structures. The AM1 computations show a broad and shallow deformation energy associated with the inter-ring twisting for all members of the series. This deformation leads to a modest barrier to rotation at the orthogonal inter-ring conformation for the parent *N*-phenylmaleimide and shifts to conformations with lower twist angles for any of the *N*-(*o*-halophenyl)maleimides. Considerable maleimide and phenyl distortions are expected for the chloro, bromo, and iodo derivatives as the inter-ring torsion angle is reduced; for these molecules and for the fluoro derivative, torsional interconversion proceeds through the perpendicular conformation. Calculations also support assignment of the ultraviolet absorption features above 250 nm to several phenyl and maleimide ring transitions. Except for the *o*-iodo derivative, the shorter wavelength features appears to be principally a phenyl $\pi \rightarrow \pi^*$ transition, while the longer wavelength feature has $\{n_\perp(O,N) + \pi_{Ph}\} \rightarrow \pi^*_{Mal}$ character. Longer wavelength absorptions in the *o*-iodo derivative may arise from overlapping $n_\perp(O,N) + \pi_{Ph} \rightarrow \sigma$(C−I, 2p−5p) transitions.

**Acknowledgment.** We thank Mr. C. Jace Pugh for experimental assistance, Dr. Jeffrey D. Zubkowski, Jackson State University, for access to diffraction equipment, and Dr. William A. Parkinson, Southeastern Louisiana University, for assistance with computations. We acknowledge support from First Chemi-

cal Corporation and Fusion UV-Curing Systems (C.W.M. and C.E.H.), the Office of Naval Research and the National Science Foundation (DUE−9250769 and DUE−9650316) (E.J.V. and D.H.M.), and Research Corporation and National Science Foundation EPSCoR (OSR-9452857) (D.H.M.).

**Supporting Information Available:** Tables 5−9 giving crystallographic data, atomic coordinates, and equivalent isotropic displacement parameters for **1**−**5**. This material is available free of charge via the Internet at http://pubs.acs.org.

## References and Notes

(1) Jönsson, S.; Sundell, P. E.; Shimose, M.; Clark, S.; Miller, C.; Morel, F.; Decker, C.; Hoyle, C. E. *Nuclear Instrum. Methods Phys. Res., Sect. B* **1997**, *131*, 276.

(2) Jönsson, S.; Ericsson, J. S.; Sundell, P. E.; Shimose, M.; Clark, S. C.; Miller, C.; Owens, J.; Hoyle, C. E. *Proc. Radtech North America '96* **1996**, *I*, 377.

(3) Clark, S. C.; Doucet, G. J.; Jönsson, E. S.; Mattson, G. A.; Hoyle, C. E. *Polym. Prepr.* **1997**, *38* (1), 178.

(4) Simose, M.; Hoyle, C. E.; Jönsson, S.; Sundell, P. E.; Owens, J.; Vaughn, K. *Polym. Prepr.* **1995**, *36* (2), 485.

(5) Jönsson, S.; Sundell, P. E.; Shimose, M.; Owens, J.; Miller, C.; Clark, S.; Hoyle, C. E. *Proc. Am. Chem. Soc., Division of PMSE*. **1996**, *74*, 319.

(6) Clark, S. C.; Jönsson, E. S.; Hoyle, C. E. U.S. Provisional Patent 60/024,546. Full patent in application.

(7) Miller, C. W.; Hoyle, C. E.; Jönsson, E. S. U.S. Provisional Patent 60/047,729. Full patent in application.

(8) Miller, C. W.; Clark, S. C.; Hoyle, C. E.; Jönsson, E. S.; Nagarajan, R.; Shao, L. U.S. Provisional Patent 60/073,100. Full patent in application.

(9) Matsuo, T. *Bull. Chem. Soc. Jpn.* **1965**, *38* (4), 557.

(10) Seliskar, C. J.; McGlynn, S. P. *J. Chem. Phys*. **1971**, *55*, 4337.

(11) *International Tables for X-ray Crystallography*; Kluwer Academic Publishers: Dordrecht, The Netherlands, 1992; Vol C.

(12) Sheldrick, G. *SHELXS-93*; Göttingen University: Göttingen, Germany, 1993.

(13) Sheldrick, G. *SHELXL-97*; Göttingen University: Göttingen, Germany, 1997.

(14) Dewar, M. J. S.; Zoebisch, E. G.; Healy, E. E. *J. Am. Chem. Soc.* **1985**, *107*, 3202.

(15) *HYPERCHEM*, release 4; Hypercube, Inc.: Waterloo, Ontario, Canada.

(16) *PC-Spartan*, version 1.1; Wave function Inc.: Irvine, CA.

(17) Ridley, J.; Zerner, M. C. *Theor. Chim. Acta* **1973**, *32*, 111.

(18) Ridley, J.; Zerner, M. C. *Theor. Chim. Acta* **1976**, *42*, 223.

(19) Frisch, M. J.; Trucks, G. W.; Schlegel, H. B.; Scuseria, G. E.; Robb, M. A.; Cheeseman, J. R.; Zakrzewski, V. G.; Montgomery, J. A., Jr.; Stratmann, R. E.; Burant, J. C.; Dapprich, S.; Millam, J. M.; Daniels, A. D.; Kudin, K. N.; Strain, M. C.; Farkas, O.; Tomasi, J.; Barone, V.; Cossi, M.; Cammi, R.; Mennucci, B.; Pomelli, C.; Adamo, C.; Clifford, S.; Ochterski, J.; Petersson, G. A.; Ayala, P. Y.; Cui, Q.; Morokuma, K.; Malick, D. K.; Rabuck, A. D.; Raghavachari, K.; Foresman, J. B.; Cioslowski, J.; Ortiz, J. V.; Stefanov, B. B.; Liu, G.; Liashenko, A.; Piskorz, P.; Komaromi, I.; Gomperts, R.; Martin, R. L.; Fox, D. J.; Keith, T.; Al-Laham, M. A.; Peng, C. Y.; Nanayakkara, A.; Gonzalez, C.; Challacombe, M.; Gill, P. M. W.; Johnson, B.; Chen, W.; Wong, M. W.; Andres, J. L.; Gonzalez, C.; Head-Gordon, M.; Replogle, E. S.; Pople, J. A. *Gaussian 98*, revision A.4; Gaussian, Inc.: Pittsburgh, PA, 1998.

(20) Becke, A. D. *J. Chem. Phys.* **1993**, *98*, 5648.

(21) Lee, C.; Yang, W.; Parr, R. G. *Phys. Rev. B* **1988**, *37*, 785.

(22) Miehlich, B.; Savin, A.; Stoll, H.; Preuss, H. *Chem. Phys. Lett.* **1989**, *157*, 200.

(23) Murray-Rust, P. *Molecular Structure and Biological Activity*; Griffin, J. F., Duax, W. L., Eds.; Elsevier: Amsterdam, The Netherlands, 1982; pp 117−131.